OPEN

Light: Science & Applications (2014) 3, e193; doi:10.1038/lsa.2014.74
© 2014 CIOMP. All rights reserved 2047-7538/14
www.nature.com/lsa

ORIGINAL ARTICLE

Multi-ion cooperative processes in Yb^{3+} clusters

Wei-Ping Qin*, Zhen-Yu Liu, Chol-Nam Sin, Chang-Feng Wu, Guan-Shi Qin, Zhe Chen and Ke-Zhi Zheng

Cooperative luminescence (CL) occurs in spectral regions in which single ions do not have energy levels. It was first observed more than 40 years ago, and all results reported so far are from a pair of ions. In this work, upconverted CL of three Yb^{3+} ions was observed in the ultraviolet (UV) region under near-infrared (NIR) excitation. The UV CL intensity showed a cubic dependence on the NIR pump power, whereas the luminescence lifetime was nearly one-third the luminescence lifetime of single Yb^{3+} ions. The triplet CL (TCL) has a clear spectral structure, in which most emission peaks are consistent with the self-convoluted spectra from single Yb^{3+} ions. Blue shifts were observed for certain peaks, indicating complex interactions among the excited Yb^{3+} ions. The probability of the TCL process *versus* the average distances among three Yb^{3+} ions was derived *via* the first- and second-order corrections to the wave functions of lanthanide ions, indicating that the formation of Yb^{3+} clusters containing closely spaced ions favors the occurrence of the multi-ion interaction processes. Furthermore, the cooperative sensitization of one Gd^{3+} ion by four excited Yb^{3+} ions (Yb^{3+}-tetramer) was demonstrated experimentally, which exhibited a novel upconversion mechanism—cluster sensitization. Our results are intriguing for further exploring quantum transitions that simultaneously involve multiple ions.

Light: Science & Applications (2014) **3,** e193; doi:10.1038/lsa.2014.74; published online 1 August 2014

Keywords: cooperative luminescence; cooperative sensitization; quantum transition; ytterbium cluster

INTRODUCTION

Cooperative luminescence (CL) usually describes the processes by which a pair of ions emits one photon by simultaneous depopulation from their excited states. It represents a special type of electronic transitions occurring in spectral regions where the individual ions do not have absorption or emission. Experimental CL results are essential clues to understanding the nature of cooperative quantum transitions, such as the energy shifts of pair levels from their parent single-ion levels, the selection rules obeyed by the cooperative transitions, and quantum entanglement in multibody systems.[1–3] The first CL was demonstrated with a pair of excited Yb^{3+} ions in 1970.[4] Since then, the CL from Yb^{3+}-dimers has been studied extensively due to their unique $4f^{13}$ configuration with two multiplets ($^2F_{5/2}$, $^2F_{7/2}$) and the relatively large absorption cross-section at ~980 nm. Various applications, such as scintillators, structural probes in solids and optical bistability, have been demonstrated with the CL from Yb^{3+}-dimers.[5–11] However, the relatively low emission cross-section impedes further experimental investigation of multi-ion cooperative processes.

Nevertheless, CL is fundamentally fascinating from a purely theoretical perspective. More than 50 years ago, Dexter explained the cooperative processes based on first-order perturbation theory,[12] in which Coulomb coupling between two ions allows for their cooperative transition as a pair of ions. For processes involving three ions simultaneously, however, Dexter concluded that it was impossible to couple triple excitations to the ground-state wave function with first-order perturbation theory, and therefore second-order corrections to the wave functions should be considered.[12] Since then, the questions have remained open whether the CL from three identical ions can be experimentally observed and what theoretical modification is needed to describe it. Here, we report the first observation of ultraviolet (UV) CL of three Yb^{3+} ions, which shows a fine spectral structure consistent with the self-convolution of the spectrum of individual Yb^{3+} ions in the near-infrared (NIR) region. We calculated its cooperative transition probabilities with first- and second-order corrections to the coupling wave functions. We further observed the sensitization of one Gd^{3+} ion by four Yb^{3+} ions in cooperation, a process involving five ions simultaneously. As a novel upconversion (UC) mechanism, the multi-ion sensitization could play important roles in multiphoton UC processes. Together, our results unambiguously confirm that cooperative quantum transition processes of more than two identical ions can occur, and we may thereby open a way to the study on multibody interactions.

MATERIALS AND METHODS

Ten millimoles of CaF_2 (99.99%) and 0.1 mmol YbF_3 (99.99%) powders (Aladdin Reagent, Shanghai, China) were used to prepare the polycrystalline. The mixed original material was heated in a platinum crucible under nitrogen atmosphere at 1500 ℃ for 3 h, then cooled to room temperature naturally. Power-adjustable continuous wave laser diodes (978 nm and 915 nm, 10 W; BWT Beijing Ltd, Beijing, China) and a Nd:YAG pulsed laser (10 Hz repetition rate, 8 ns pulse width; Quanta-ray, Spectra-Physics, CA, USA) equipped with second harmonic generation, third harmonic generation, fourth harmonic generation and Raman shifter were employed as the pump sources for spectral analysis. The luminescence spectra were recorded with an 1-m

State Key Laboratory on Integrated Optoelectronics, College of Electronic Science and Engineering, Jilin University, Changchun 130012, China
Correspondence: Professor WP Qin, State Key Laboratory on Integrated Optoelectronics, College of Electronic Science and Engineering, Jilin University, 2699 Qianjin Street, Changchun 130012, China
E-mail: wpqin@jlu.edu.cn

Received 27 February 2014; revised 25 April 2014; accepted 28 April 2014

monochromator (SPEX 1000M, model: 232/488MSD; HORIBA Jobin Yvon Inc., Edison, NJ, USA) equipped with a 600 lines mm^{-1} (for NIR and visible fluorescence) grating or an 1800 lines mm^{-1} (for UV fluorescence) grating. The pulse signal from the spectrophotometer was connected to a boxcar averager (Model 162; Princeton Applied Research, Oak Ridge, TN, USA). The boxcar output was fed continuously to a PC equipped with a Jobin Yvon SpectrAcq2 data acquisition system. The spectral measurements at low temperature were performed using a helium-cycled cryostat (ARS-2HW; Advanced Research Systems, Macungie, PA, USA). A digital oscilloscope (DPO4104B, bandwidth 1 GHz, sampling rate 5 GS s^{-1}; Tektronix, Shanghai, China) was used to record the decay curves.

RESULTS AND DISCUSSION

Optical characteristics of cooperative luminescence

The observation was performed with CaF_2:1%Yb^{3+} polycrystalline powders (see also Supplementary Figs. S1, S2 and S3). Under the excitation of a 978 nm NIR laser, the CaF_2:1%Yb^{3+} sample showed bright green luminescence at room temperature. Spectral analysis indicated that the bright-green UC emission came from Yb^{3+}-dimers in the CaF_2:Yb^{3+} polycrystalline, as shown in Figure 1a (black line). More importantly, an emission band in the UV region was observed at room temperature, as shown in Figure 1b (black line). The UV emission band centered at ~343 nm was approximately 2×10^4 times (see also Supplementary Table S1 and Supplementary Figs. S4 and S5) weaker than the bright green emission. The emission spectrum of Yb^{3+}-dimers was obtained under the same excitation and collection conditions as the UV emission band, but a combination of three neutral density filters with a total transmittance of 0.75% were placed in front of the collection entry of the monochromator so that the emission intensities were in the linear range of the instrument. Based on the transmittance of the filters, the emission intensity was back-calculated after integrating the emission spectrum over the wavelength range. The photon energy of the UV emission band is nearly triple the NIR photon energy emitted by individual Yb^{3+} ions, indicating that the UV luminescence is most likely due to the cooperatively radiative transition of three excited Yb^{3+} ions in the following manner:

$$\begin{aligned}&\mathrm{Yb}^{*}\left({}^{2}F_{5/2}\right)+\mathrm{Yb}^{*}\left({}^{2}F_{5/2}\right)+\mathrm{Yb}^{*}\left({}^{2}F_{5/2}\right)\rightarrow\\&\mathrm{Yb}\left({}^{2}F_{7/2}\right)+\mathrm{Yb}\left({}^{2}F_{7/2}\right)+\mathrm{Yb}\left({}^{2}F_{7/2}\right)+h\nu\end{aligned}\tag{1}$$

A cooperative emission spectrum of Yb^{3+}-dimers is formed from all energetic combinations of two transitions between the Stark levels of the ${}^2F_{5/2}$ and the ${}^2F_{7/2}$ manifolds.[8] Therefore, the CL spectra $F_{\mathrm{Dimer}}(\lambda)$ and $F_{\mathrm{Trimer}}(\lambda)$ of Yb^{3+}-dimers and Yb^{3+}-trimers can be calculated from the spectrum $f(\lambda)$ of individual Yb^{3+} ions in the NIR region (Figure 1a, blue line) by self-convolution:

$$F_{\mathrm{Dimer}}(\lambda)=\int_{-\infty}^{\infty}f(\lambda')f(\lambda-\lambda')\mathrm{d}\lambda'\tag{2}$$

and

$$\begin{aligned}F_{\mathrm{Trimer}}(\lambda)&=\int_{-\infty}^{\infty}f(\lambda')F_{\mathrm{Dimer}}(\lambda-\lambda')\mathrm{d}\lambda'\\&=\int_{-\infty}^{\infty}\int_{-\infty}^{\infty}f(\lambda')f(\lambda'')f(\lambda-\lambda'-\lambda'')\mathrm{d}\lambda''\mathrm{d}\lambda'\end{aligned}\tag{3}$$

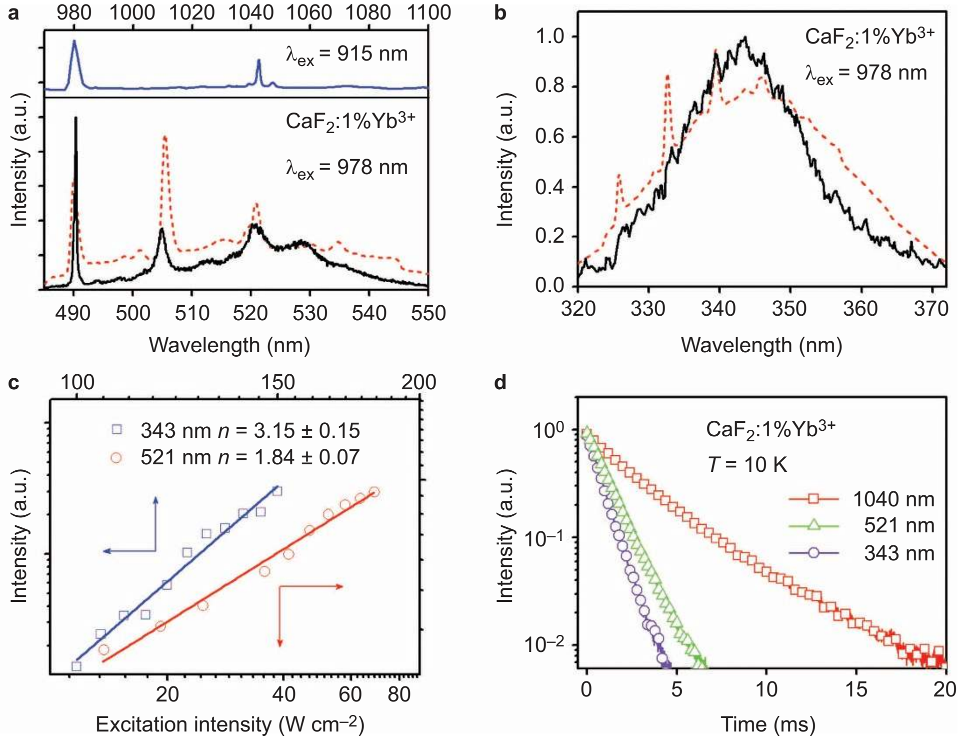

Figure 1 (**a**) Green CL spectrum (black line) and the self-convolution (red short dash line) of the infrared luminescence spectrum (blue line) of Yb^{3+}-doped CaF_2 polycrystalline. The blue spectrum was measured at low temperature (10 K) under excitation by a 915 nm laser diode. (**b**) UV CL spectrum (black line) and the triple self-convolution of infrared luminescence spectrum (**a**, blue line) of Yb^{3+}-doped CaF_2 polycrystalline under 978 nm laser excitation (~120 W cm^{-2}). (**c**) Log–log plots of CL intensity as a function of pump power of the 978 nm laser. (**d**) Fluorescence decay curves of 1040 nm (2.88 ms), 521 nm (1.23 ms) and 350 nm (0.84 ms) emissions from single Yb^{3+} ions, Yb^{3+}-dimers and Yb^{3+}-trimers in CaF_2 polycrystalline, respectively. CL, cooperative luminescence; ex, excitation; UV, ultraviolet.

The calculated self-convoluted spectra of Yb^{3+}-dimers and trimers are plotted as red short dashed lines in Figure 1a and 1b, respectively. It is noted that each of the self-convoluted spectra is in good agreement with the experimentally observed spectra.

In principle, the upconverted CL intensity I_f is proportional to the n^{th} power of the NIR excitation intensity I_{NIR}, i.e., $I_f \propto I_{\mathrm{NIR}}^n$, where n is the number of Yb^{3+} ions involved per high-energy photon emitted.[13] While the measured intensity of the green emission shows a quadratic dependence (Figure 1c), the UV emission is cubically dependent on the excitation power, indicating that the UV emission originates from the simultaneous de-excitation of three Yb^{3+} ions (Yb^{3+}-trimer). However, the luminescence intensity $I_i(t)$ of the individual ions is expressed by $I_i(t) \propto n_i(t) = n_i(0)\exp(-t/\tau_i)$, where $n_i(t)$ is the number of excited ions at time t. For the CL from Yb^{3+}-dimers, $n_d(t) = n_d(0)\exp(-t/\tau_d)$, where $n_d(t)$ is the number of excited dimers at time t. The value of $n_d(t)$ is proportional to $[n_i(t)]^2$,[4] and therefore, $\tau_d = \tau_i/2$. Similarly, it is inferred that $n_t(t)$ for the TCL of Yb^{3+}-trimers is proportional to $[n_i(t)]^3$, and therefore $\tau_t = \tau_i/3$. Figure 1d shows the fluorescence decay curves recorded at 1040 nm, 521 nm and 343 nm, respectively. Each curve can be fitted with a single exponential function. The lifetime of the green emission (521 nm) is 1.23 ms, nearly half (43%) of the lifetime of individual Yb^{3+} ions (2.88 ms). The lifetime (0.84 ms) of the UV emission (343 nm) is approximately one-third (29%) of the lifetime for the single Yb^{3+} ions. These results confirm that the newfound UV emission originates from cooperatively radiative transition of three excited Yb^{3+} ions.

Energy shifts of cooperative luminescence

Low-temperature high-resolution spectroscopy was performed to investigate the fine CL spectral structures of Yb^{3+}-dimers and trimers. At 1-mol% dopant concentration, Yb^{3+} ions in CaF$_2$ prefer to form hexameric clusters, in which Yb^{3+} ions substitute for Ca^{2+} ions and are situated in nearly tetragonal crystal-field environments.[14] The excess impurity charge (+1) of the Yb^{3+} cations is compensated primarily by embedding additional F$^-$ ions in the anion sublattice interstices. The $^2F_{5/2}$ and $^2F_{7/2}$ states of Yb^{3+} ions split into three and four Stark components in a tetragonal crystal field, respectively (Figure 2a).[15] The NIR spectrum from individual Yb^{3+} ions, the visible spectrum from Yb^{3+}-dimers, and the UV spectrum from Yb^{3+}-trimers recorded at low temperature (10 K) are depicted in Figure 2b–2d. The emission spectrum of single Yb^{3+} ions in CaF$_2$ consists of three main peaks located at 980 nm (A), 1040 nm (B) and 1069 nm (C) and of weak peaks, which most likely originate from the transitions between Stark levels (Figure 2b). Each of the self-convoluted spectra (red short dash lines in Figure 2c and 2d) is in agreement with its corresponding CL spectrum. The CL spectrum of Yb^{3+}-dimers (Figure 2c) shows a set of peaks (AA, BB, CC and DD) that almost doubles the energy of the peaks (A, B, C and D, respectively) in the NIR spectrum. Certain other peaks (e.g., AB, AC and BC) correspond to the sum of the energies of two different NIR peaks (e.g., A, B and C). These visible emissions can be clearly identified as the CL from the simultaneous de-excitation of two excited Yb^{3+} ions.

The UV TCL from three excited Yb^{3+} ions also shows a clear fine structure that is consistent with the self-convoluted spectrum of individual Yb^{3+} ions in the NIR region. The emission peaks marked by AAA, BBB and CCC correspond to the triple energy of the emission peaks (A, B and C) of individual Yb^{3+} ions, respectively. The other TCL peaks (e.g., AAB, ABB, ABC and ACC) are due to the cooperation of different radiative transitions (e.g., A, B, C and D) in the NIR region. As indicated in Figure 2d, some experimental TCL peaks (such as ABB

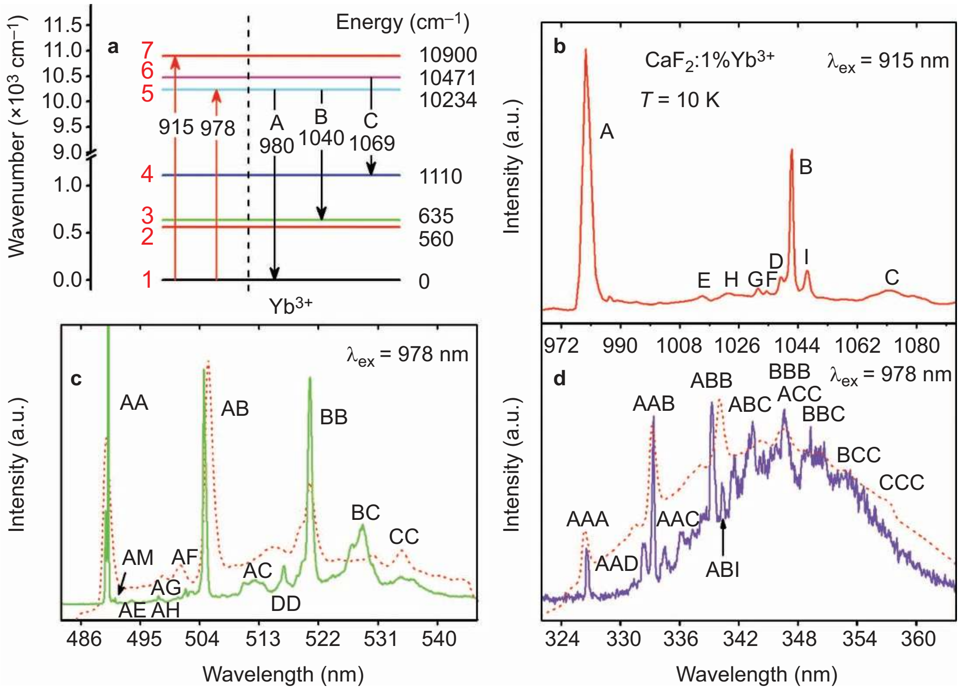

Figure 2 (**a**) Energy-level scheme for Yb^{3+} ions in tetragonal crystal-field environments. Emission spectra of CaF$_2$:1%Yb^{3+} in the regions of (**b**) NIR (the same as the NIR emission spectrum in Figure 1), (**c**) visible and (**d**) UV, respectively, recorded at 10 K. The emission peaks with alphabetical combinations in **c** and **d** represent the corresponding relationships between these peaks and the emission bands in **b**. The red short dashed lines represent the corresponding self-convolution spectra of the NIR emission spectrum under 915 nm laser diode excitation **b** (the same as in Figure 1a and 1b, red short dashed lines, respectively). CL, cooperative luminescence; ex, excitation; NIR, near-infrared.

and ABC) of Yb^{3+}-trimers showed obvious blue shifts in comparison with the peaks in the self-convoluted spectrum. Interestingly, the energy shift occurred primarily in the coupling of different excited sublevels, while the coupling of the same excited sublevels (such as AAA and BBB) displayed no changes in their cooperative transition energies. These observations reveal that the triplet cooperative transition occurs with complex interactions among the clustered Yb^{3+} ions even though their wave functions do not overlap.

Theoretical calculations of the cooperative transition probability for Yb^{3+}-trimers

Previously, Kushida had obtained the cooperative transition probability for Yb dimers under first-order perturbation.[16] However, in the case of Yb^{3+}-trimers, the first-order contribution of the electric dipole moment to cooperative optical luminescence vanishes through term-by-term cancellations. Thus, the second-order contributions of the electronic dipole moment should be considered. To calculate the cooperative optical luminescence of Yb^{3+}-trimers, we write the initial state, intermediate state, and final state as $a_1b_1c_1$, $a'b'c'$and $a_2b_2c_2$, respectively. The functions $\psi_n^{(0)}$,$\psi_n^{(1)}$, and $\psi_n^{(2)}$are the zero-, first- and second-order corrected wave functions, respectively, and thus, the second-order contributions of the electronic dipole moment should be

$$\langle\psi^{(1)}_{a_1b_1c_1}|D^{(1)}_m|\psi^{(1)}_{a_2b_2c_2}\rangle+\langle\psi^{(0)}_{a_1b_1c_1}|D^{(1)}_m|\psi^{(2)}_{a_2b_2c_2}\rangle+\langle\psi^{(2)}_{a_1b_1c_1}|D^{(1)}_m|\psi^{(0)}_{a_2b_2c_2}\rangle$$

The first term indicates that first-order corrections to the wave function could contribute to the second-order contribution of the electric dipole moment. The second-order contributions between the initial state and final state through the interaction $H_{\mathrm{AB}}+H_{\mathrm{AC}}+H_{\mathrm{BC}}$ have many multipole terms such as *dd–dd*, *dq–dd*, *dd–qq*, *dq–dq*, *dq–qq* and *qq–qq*. The lowest order term of parity-allowed interactions is *dq–dd* (*dd–dq*) and can be written as follows:

$$\begin{aligned}M_m&=\langle a_1b_1c_1\big|D^{(1)}_m\big|a_2b_2c_2\rangle\\&=\sum_{a'b'}\frac{\langle a'c_1|H_{\mathrm{AC}}|a_2c_2\rangle}{E_{a_1b_1c_1}-E_{a_2b'c_2}}\frac{\langle a_1b_1|H_{\mathrm{AB}}|a'b'\rangle}{E_{a_1b_1}-E_{a'b'}}\langle b'\big|D^{(1)}_m\big|b_2\rangle\\&+\sum_{a'c'}\frac{\langle a'c_1|H_{\mathrm{AC}}|a_2c'\rangle}{E_{a_1b_1c_1}-E_{a_2b_2c'}}\frac{\langle a_1b_1|H_{\mathrm{AB}}|a'b_2\rangle}{E_{a_1b_1}-E_{a'b_2}}\langle c'\big|D^{(1)}_m\big|c_2\rangle\\&+34\text{ similar terms}\end{aligned}\tag{4}$$

The terms in Equation (4) can be expanded using a tensor operator, which can be found in many papers.[16–18]

$$\begin{aligned}M_m=&\sum\frac{600}{R^7}C^{12}_{q_1q_2}(\theta_1,\phi_1)C^{11}_{q_3q_4}(\theta_2,\phi_2)(-1)^{q+q'}\begin{pmatrix}1&2&1\\q_1&-q&m\end{pmatrix}\\&\times\langle J_1M_1\big|U^{(2)}_q\big|J_2M_2\rangle\Xi^2(1,2)\langle 4f\big|r^2\big|4f\rangle\langle f\big\|C^{(2)}\big\|f\rangle\\&\times\langle J_1M_1\big|U^{(2)}_{q_2}\big|J_2M_2\rangle\begin{pmatrix}1&2&1\\q_3&-q'&q_4\end{pmatrix}\langle J_1M_1\big|U^{(2)}_{q'}\big|J_2M_2\rangle\end{aligned}\tag{5}$$

where we assumed that $R_{\mathrm{AB}}\approx R_{\mathrm{AC}}\approx R_{\mathrm{BC}}\approx R$ and

$$\Xi(k_1,k)=\sum_{n'l'}\begin{Bmatrix}1&k&k_1\\f&l'&f\end{Bmatrix}\langle 4f|r|n'l'\rangle\langle n'l'|r^{k_1}|4f\rangle\langle f\big\|C^{(1)}\big\|l'\rangle\langle l'\big\|C^{(k_1)}\big\|f\rangle/\Delta E$$

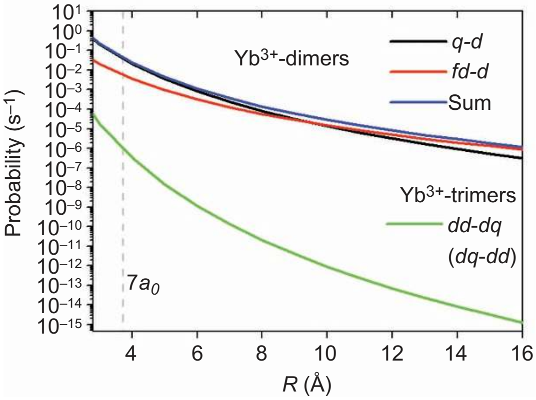

Figure 3 Dependence of cooperative emission probabilities on distance R of interacting ions in CaF$_2$ polycrystalline. For Yb^{3+}-dimers, red line: the *fd–d* interaction, blue line: the *q–d* interaction and black line: the sum of the two. For Yb^{3+}-trimers, green line: *dd–qd* (or *qd–dd*) interaction. The value a_0 is the Bohr radius.

If we take an average of the initial state and sum over all the components in the final state, we obtain

$$\begin{aligned}&\left[M^2_{\mathrm{trimer}}\right]_{dd-dq}=\\&\sum_m\overline{M_m{}^2}=\frac{14400}{(2J_1+1)^3}\left(\frac{1}{R^7}\right)^2\langle J_1\big\|U^{(2)}\big\|J_2\rangle^6\Xi^4(1,2)\langle 4f\big|r^2\big|4f\rangle^2\langle f\big\|C^{(2)}\big\|f\rangle^2\end{aligned}\tag{6}$$

Therefore, the transition probability of the cooperative luminescence of Yb^{3+}-trimers can be calculated by substituting $\left[M^2_{\mathrm{trimer}}\right]_{dd-dq}$ into Equation (7)[16]

$$W=\frac{e^2}{4\pi\varepsilon_0}\frac{4\omega^3}{3\hbar c^3}\frac{n(n^2+2)^2}{9}M^2\tag{7}$$

The result is 1.01×10^{-6} s^{-1}, by using R=7a_0, where a_0 is the Bohr radius.

The contributions of *dd–dd*, *dd–qq*, *dq–dq*, *dq–qq* and *qq–qq* can be calculated similarly as above. The results show that these contributions are, respectively, at least two orders of magnitude smaller than the contributions due to the *dd–dq* (or *dq–dd*) mechanism. Meanwhile, based on Kushida's result,[16] the transition probability of Yb^{3+}-dimers in CaF$_2$ polycrystalline is 3.9×10^{-2} s^{-1}. The probability ratio of Yb trimers to dimers is $W_{\mathrm{dimers}}/W_{\mathrm{trimers}}=3.87\times10^4$. We plotted the curves for the probability of the CL processes versus the average distances among three Yb^{3+} ions, as shown in Figure 3. Experimentally, the transition probability ratio of Yb^{3+}-dimers and Yb^{3+}-trimers was approximately 2×10^4 (Supplementary Table S1), which is approximately consistent with our theoretical result. Theoretical calculation indicates the formation of Yb^{3+} clusters containing closely spaced ions to favor the occurrence of multi-ion cooperative processes. The theoretical result also indicated that the multi-ion cooperative processes could occur in the regime of both the first- and second-order corrections to the wave functions of lanthanide ions.

Sensitization of one Gd^{3+} ion by four Yb^{3+} ions in cooperation

We further observed the sensitization of one Gd^{3+} ion by four Yb^{3+} ions in cooperation, a process involving five ions simultaneously. The UC spectra of CaF$_2$:Yb^{3+}, CaF$_2$:Gd^{3+}, and CaF$_2$:Yb^{3+}, Gd^{3+} upon 978 nm excitation are shown in Figure 4a. The emission peak at 342.8 nm is attributed to the TCL from the Yb^{3+}-trimers, and the emission peak at 314.8 nm is attributed to the radiative transition

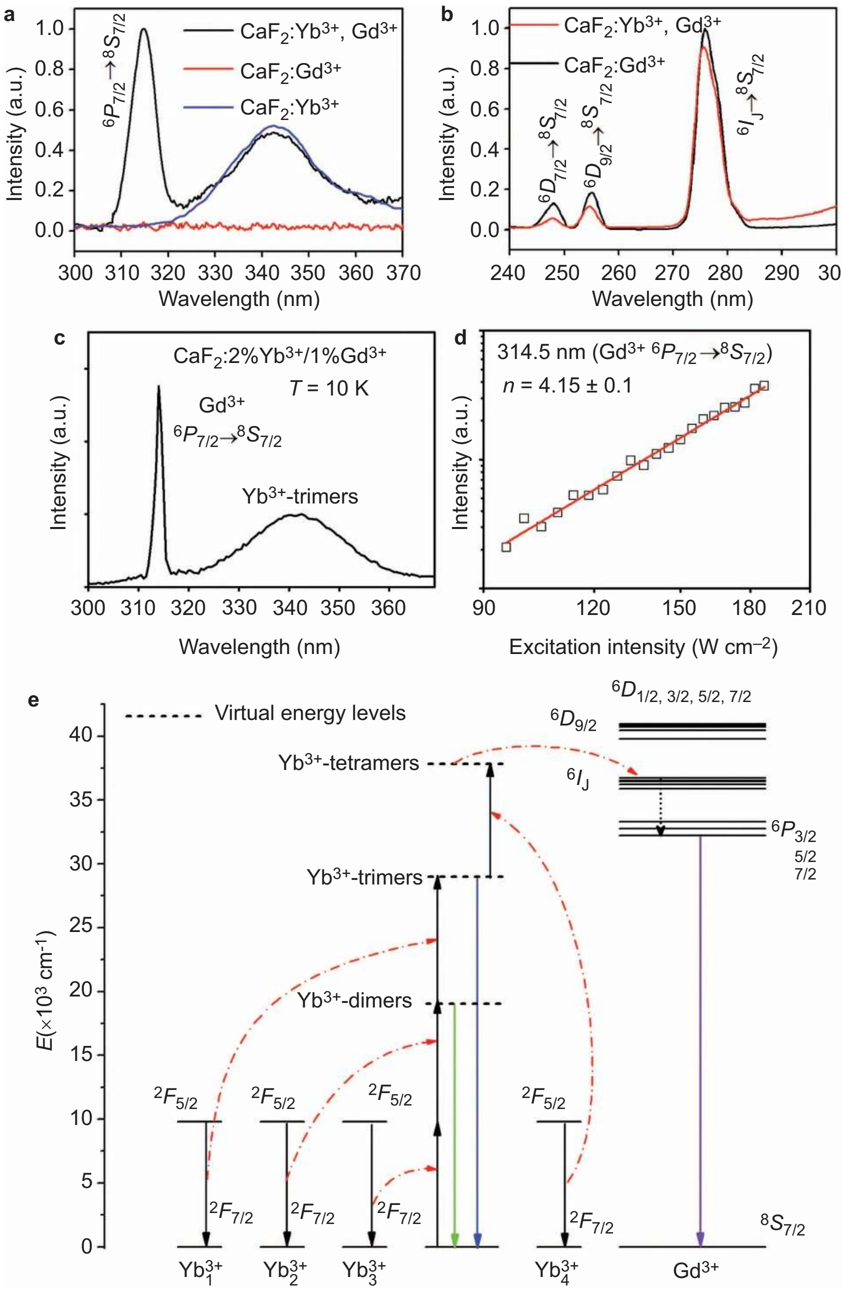

Figure 4 Characterizations of cooperative energy transfer from Yb^{3+} clusters to Gd^{3+} ions. (**a**) Upconversion spectra of $CaF_2:Yb^{3+}$, $CaF_2:Gd^{3+}$ and $CaF_2:Yb^{3+}$, Gd^{3+} upon 978 nm excitation. (**b**) Excitation spectra (λ_{em}=314.5 nm, Gd^{3+}: $^6P_{7/2}\rightarrow{}^8S_{7/2}$) of $CaF_2:Gd^{3+}$ and $CaF_2:Yb^{3+}$, Gd^{3+}. (**c**) Upconversion emission spectrum of CaF_2:2%Yb^{3+}, 1%Gd^{3+} upon 978 nm excitation (~150 W cm^{-2}) at 10 K and (**d**) excitation power dependence of 314.5 nm emission from Gd^{3+} ions in CaF_2:2%Yb^{3+}, 1%Gd^{3+}. (**e**) Schematic energy level diagrams of Yb^{3+} and Gd^{3+}. The cooperative energy transfer from four excited Yb^{3+} ions to one Gd^{3+} ion is shown by red dash-dot arrows. Green, blue, and purple arrows indicate the emission processes of Yb^{3+}-dimers, Yb^{3+}-trimers and Gd^{3+} ions, respectively. The black dot arrow indicates the non-radiative relaxation from ^6I_J to $^6P_{7/2}$ of Gd^{3+} ions.

of $^6P_{7/2}\rightarrow{}^8S_{7/2}$ (Gd^{3+}). No UC emission was recorded for $CaF_2:Gd^{3+}$, demonstrating that multiple 978 nm photons cannot excite Gd^{3+} ions directly. The excitation spectra, shown in Figure 4b, confirmed that the population of $^6P_{7/2}$ comes from the upper energy levels of Gd^{3+} ions in $CaF_2:Yb^{3+}$, Gd^{3+}. As no other rare earth ions were doped but Yb^{3+}, Gd^{3+}, and no emission was observed from impurity, a special energy transfer mechanism from Yb^{3+} ions to Gd^{3+} ions occurred. As we have observed the TCL band in the UV region, it is reasonable to infer that the sensitization of the Gd^{3+} ions originates from the Yb^{3+} clusters. The energy gap of Gd^{3+} between the ground state $^8S_{7/2}$ and the first excited state $^6P_{7/2}$ is 32 000 cm^{-1}. Thus, the ion number of the Yb^{3+} clusters must be no less than three, as the energy mismatch between the excited state ($^2F_{5/2}$) and the ground state ($^2F_{7/2}$) is approximately 9400–10900 cm^{-1}. First, for Yb^{3+}-trimers, the energy gap between the center of TCL band and the first excited state $^6P_{7/2}$ of Gd^{3+} is ~2642 cm^{-1}, and thus the assistance of phonons is necessary. Because the phonon energy of CaF_2 is approximately 324 cm^{-1},[19] eight phonons are necessary to facilitate the population of $^6P_{7/2}$ of Gd^{3+}. However, this large energy mismatch results in an extremely low probability of the energy transfer process. Figure 4c shows the UC emission spectrum of CaF$_2$:2%Yb^{3+}, 1%Gd^{3+} at 10 K. The emission bands showed narrowing, but the relative intensity of the 314.8 nm emission to the Yb^{3+}-trimers does not decrease compared with that obtained at room temperature. As is well known, at low temperature, the phonon effect should be reduced significantly with the energy transfer from excited Yb^{3+}-trimers. Therefore, the first sensitizing route is proved to be irrational.

For Yb^{3+}-tetramers, their excited states are located in the UV region overlapping with the excited state ^6I_J of Gd^{3+} ions, though their emission has not been observed. Clusters of rare earth ions, including dimers and larger aggregates, are very common in crystals and glasses even at extremely low dopant concentrations.[20] For a UC process, the emission intensity I_f is proportional to the n^{th} power of the NIR excitation intensity I_{NIR}, i.e., $I_f \propto I_{\text{NIR}}^n$, where n is the number of NIR photons absorbed per upconverted photon emitted.[13] Figure 4d shows the pump-power dependences of the UC emission of Gd^{3+}, and the n value was 4.15 ± 0.1 for the 314.8 nm emission peak, indicating that the UV emission came from the sensitization and simultaneous de-excitation of four Yb^{3+} ions (Yb^{3+}-tetramers). The ^6I_J of Gd^{3+} ions is sensitized by the excited Yb^{3+}-tetramers, and then through nonradiative decay, the excited Gd^{3+} ions relaxes to the first excited state $^6P_{7/2}$, which results in the 314.8 nm UV emission peak in the CaF$_2$:Yb^{3+}, Gd^{3+} system. Figure 4e shows the schematic energy level diagrams of Yb^{3+}, Gd^{3+}, and the possible cooperative energy transfer and upconverted emission processes. This process involves five ions in close proximity to produce one UV photon, much more complex than the general electronic transitions in isolated ions.

CONCLUSIONS

In summary, multi-ion cooperative processes were observed from Yb^{3+} clusters in CaF$_2$ matrix. Under NIR excitation, UV emissions from Yb^{3+}-doped CaF$_2$ correspond to the CL of three Yb^{3+} ions. Low-temperature laser spectroscopy clearly shows spectral structures that are in good agreement with the self-convoluted spectra of single Yb^{3+} ions. We further observed a UV emission from Gd^{3+} ions in a Yb^{3+}, Gd^{3+}-codoped sample under NIR excitation, for which the mechanism is ascribed to the sensitization of Gd^{3+} by four excited Yb^{3+} ions in cooperation. This proposal is a novel UC mechanism, and multi-ion sensitized processes could play important roles in multiphoton UC. Theoretical calculation indicates that the Yb^{3+} ions tend to form clusters to favor the occurrence of these multi-ion cooperative processes and also indicates that the second-order contributions of the electronic dipole moment could allow such multi-ion cooperative processes. Our results show that multi-ion clusters could be an ideal model for further exploration of quantum transitions that simultaneously involve multiple ions.

ACKNOWLEDGMENTS

This work was supported by the National Natural Science Foundation of China (Grants 61178073, 11274139, 61222508 and 61275189).

---

1 Balslev E, Combes JM. Spectral properties of many-body Schrödinger operators with dilatation–analytic interactions. *Commun Math Phys* 1971; **22**: 280–294.
2 Auzel F. Upconversion and anti-stokes processes with f and d ions in solids. *Chem Rev* 2004; **104**: 139–174.
3 Amico L, Fazio R, Osterloh A, Vedral V. Entanglement in many-body systems. *Rev Mod Phys* 2008; **80**: 517–576.
4 Nakazawa E, Shionoya S. Cooperative luminescence in YbPO$_4$. *Phys Rev Lett* 1970; **25**: 1710–1712.
5 Nakazawa E. Cooperative optical transitions of Yb^{3+}–Yb^{3+} and Gd^{3+}–Yb^{3+} ion pairs in YbPO$_4$ hosts. *J Lumin* 1976; **12–13**: 675–680.
6 Auzel F. Upconversion processes in coupled ion systems. *J Lumin* 1990; **45**: 341–345.
7 Hehlen MP, Kuditcher A, Rand SC, Lüthi SR. Site-selective, intrinsically bistable luminescence of Yb^{3+} ion pairs in CsCdBr$_3$. *Phys Rev Lett* 1999; **82**: 3050–3053.
8 Schaudel B, Goldner P, Prassas M, Auzel F. Cooperative luminescence as a probe of clustering in Yb^{3+} doped glasses. *J Alloys Compd* 2000; **300–301**: 443–449.
9 de la Rosa E, Solis D, Díaz-Torres LA, Salas P, Angeles-Chavez C *et al*. Blue-green upconversion emission in ZrO$_2$:Yb^{3+} nanocrystals. *J Appl Phys* 2008; **104**: 103508.
10 Boulon G. Why so deep research on Yb^{3+}-doped optical inorganic materials? *J Alloys Compd* 2008; **451**: 1–11.
11 Chen D, Yu Y, Huang P, Weng F, Lin H *et al*. Optical spectroscopy of Eu^{3+} and Tb^{3+} doped glass ceramics containing LiYbF$_4$ nanocrystals. *Appl Phys Lett* 2009; **94**: 041909.
12 Dexter DL. Cooperative optical absorption in solids. *Phys Rev* 1962; **126**: 1962–1967.
13 Pollnau M, Gamelin DR, Lüthi SR, Güdel HU, Hehlen MP. Power dependence of upconversion luminescence in lanthanide and transition-metal-ion systems. *Phys Rev B* 2000; **61**: 3337–3346.
14 Petit V, Camy P, Doualan JL, Portier X, Moncorgé R. Spectroscopy of Yb^{3+}:CaF$_2$: from isolated centers to clusters. *Phys Rev B* 2008; **78**: 085131.
15 Weber MJ, Bierig RW. Paramagnetic resonance and relaxation of trivalent rare-earth ions in calcium fluoride. I. Resonance spectra and crystal fields. *Phys Rev* 1964; **134**: A1492.
16 Kushida T. Energy transfer and cooperative optical transitions in rare-earth doped inorganic materials. I. Transition probability calculation. *J Phys Soc Jpn* 1973; **34**: 1318–1326.
17 Goldner P, Pellé F, Meichenin D, Auzel F. Cooperative luminescence in ytterbium-doped CsCdBr$_3$. *J Lumin* 1997; **71**: 137–150.
18 Goldner P, Schaudel B, Prassas M. Dependence of cooperative luminescence intensity on Yb^{3+} spatial distribution in crystals and glasses. *Phys Rev B* 2002; **65**: 054103.
19 Tu J, FitzGerald SA, Campbell JA, Sievers AJ. Glass-like properties observed in low-frequency Raman scattering of mixed fluorite crystals. *J Non-Cryst Solids* 1996; **203**: 153–158.
20 Catlow CR, Chadwick AV, Greaves GN, Moroney LM. Direct observations of the dopant environment in fluorites using EXAFS. *Nature* 1984; **312**: 601–604.

Supplementary information for this article can be found on the *Light: Science & Applications*' website (http://www.nature.com/lsa/)

doi:10.1038/lsa.2014.74